Chapter 2

Literature Survey

Since the early 2000s, various works have been underway on automatic detection and identification of parasite eggs. Researchers are actively working in this area, to address various issues and challenges. In this chapter, an extensive review of notable prior works is drawn by studying their methodologies and effectiveness in detecting and identifying various types of parasite eggs in microscopic images. The review work is divided into three sections: segmentation, feature extraction and classification, and CNN-based object detection. These sections are described as follows:

2.1 Parasite Egg Segmentation

There are many different types of image segmentation methods, such as thresholding, edge detection, region-based, clustering-based, graph-based, etc., that can be used in various computer vision applications. However, the literature shows some common techniques that are employed for the segmentation of images containing parasite eggs. A classification of these methods based on their working principles is shown in Figure 2-1 and discussed about the same in the following subsections. These methods are used in various ways for segmenting different kinds of microscopic images of parasite eggs.

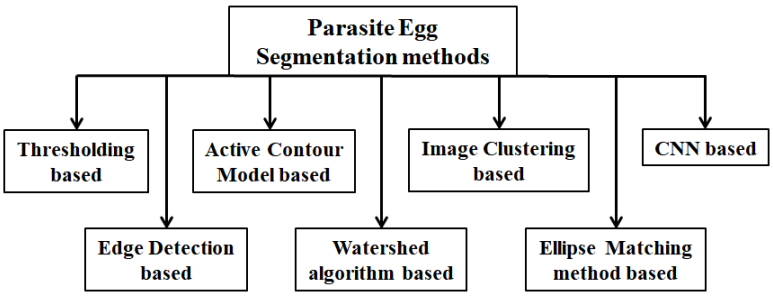

Figure 2-1: Methods used for Parasite Egg Segmentation

2.1.1 Threshodling Based Approaches

Image thresholding is one of the most popular and simplest methods for digital image segmentation [24]. The operation uses a threshold value to produce a binary image from the grayscale that represents the foreground objects. Normally, pixel values higher than the threshold are considered as foreground objects and others represent background. Depending on the way of choosing the threshold value, the image thresholding method can be divided into two subgroups, namely global thresholding and local thresholding [23]. In global thresholding, a constant threshold value is selected, which is applied for the entire image [23, 31]. The process of global thresholding can be defined as shown in equation 2.1.

$$O(x,y) = \begin{cases} 1, & \text{if I(x, y)} > \text{T} \\ 0, & \text{if I(x, y)} \leq \text{T} \end{cases} \tag{2.1}$$

Where, *I(x, y)* is the function of pixel intensity values of an input image and *O(x, y)* is the output image [24]. Threshold value T can be chosen manually from the prior knowledge of pixel intensity distribution or the grayscale intensity histogram of the input image. Several methods can be used to automatically calculate the threshold value from images. Among all of them, Otsu's method is considered one of the most effective, and it is commonly used in many segmentation tasks [23]. In contrast with the global thresholding technique, local thresholding uses multiple threshold values for the different parts of an image [23, 31]. An entire image is divided into multiple sub-images, and a threshold value is calculated for each sub-image to perform the thresholding process. The threshold value for a local region can be calculated manually or automatically based on the intensity distribution of that region.

In 2001, Y. S. Yang et al. [9] used the global thresholding method to segment seven different species of human helminth parasite eggs in digital micro-

scopic images of fecal matter. They choose the threshold value as 35% of the maximum pixel intensity level of an input image. This threshold value was determined using the intensity histograms which have bimodal distribution in most of the cases and their valley points co-occur at that level [9]. After thresholding, some unwanted objects were eliminated from the resultant binary images based on the minimum size of the parasite eggs. Finally, the internal holes of the remaining objects were filled using a method called multi-directional inward region growing [9]. Image thresholding technique was also used by Cesar A. B. Castanon et al. [32] for the segmentation of microscopic images containing seven types of parasite eggs. In their experiment, they used only the images that contained a single parasite egg with no other impurities. These images were cropped manually from the larger microscopic images containing multiple eggs. Hence, they used only the binary thresholding method with the threshold value calculated manually from each input image. E. Dogantekin et al. [33] also applied global thresholding to perform the segmentation of sixteen types of human parasite egg images. Image noise was reduced using median filtering, and contrast was enhanced before the segmentation process so that the thresholding operation performed better [33]. In their work, the midpoint of the gray-level histogram of an input image was chosen as the threshold value. After the thresholding, a few morphological operations, such as erosion, dilation, and filling holes, were applied to remove some unwanted patterns and fill the holes in the segmented parasite eggs. Derya Avci et al. [34] used a similar segmentation approach with some pre-processing steps such as noise reduction and enhancement of image contrast. Alicia Alva et al. [35] also used contrast enhancement and reduction of background noise operations on the microscopic images of stool samples containing eggs of Taenia sp., Fasciola hepatica, Diphyllobothrium latum, and Trichuris trichiura. Then the global binarization method was applied to perform the segmentation task on these images. Since the images contain only a single parasite egg, it was sufficient to use only the global binarization or thresholding process. However, border smoothing, exclusion of boundary objects, and filling holes were used as post-processing steps for better output. Johan. M. Bruun et al. [36] used a fixed threshold value of 135, to perform segmentation of Trichuris suis parasite eggs in bright field microscopic images. The authors stated that their entire image acquisition process was performed with controlled illumination, and hence a fixed threshold value works best on the effect of image content in the segmentation process. S. M. Sulong et al. [37] also performed global thresholding on the microscopic images containing Ascaris lumbricoides parasite eggs with the threshold value calculated using Otsu's method [38].

In many cases, only the thresholding operation is insufficient for proper segmentation of the images. Depending on the appearance of different objects in the images, some other operations may be required in addition to the thresholding process. Md. A. E. Abdalla and H. Seker [39] applied the Moore-Neighbour Tracing (MNT) method after global thresholding for segmentation of Eimeria parasite eggs. The MNT method was used to accurately find the egg boundaries in the binary images. In their work, the threshold value was calculated automatically using Otsu's algorithm [38] for all the images they used. In a recent work from S. V. Inacio et al., [40] for automatic diagnosis of Canine Gastrointestinal parasites, the thresholding method was used to segment four types of parasite eggs in microscopic fecal sample images of dogs. After the thresholding operation, an ellipse fitting method was applied in the binary images to filter different objects based on the area, pixel connectivity, symmetry, perimeter, and length of the major and minor axes of the best-fitted ellipse with the objects. Various research works that used the image thresholding process with different types of parasite egg images are shown in Table 2.1.

Table 2.1: Parasite egg segmentation works that use Thresholding based method

Paper	**Type of Images**	**Species of Parasite eggs**
Y. S. Yang et al. [9], 2001	Total 82 microscopic Fecal sample images containing parasite eggs and debris	Helminth eggs: Ascaris lumbricoides, Trichuris trichiura, Capillaria, Philippinensis, Clonorchis sinensis, Paragonimus westermani, Diphyllobothrium latum Taneia
C. Castanon et al. [32], 2017	3891 images that contained only a single egg	Seven types of Eimeria oocysts: E. Maxima, E. brunetti, E. tenella, E. necatrix, E. praecox, E. acervulina, E. mitis

Table 2.1: (Continued)

Paper	**Type of Images**	**Species of Parasite eggs**
E. Dogantekin et al. [33], 2008	Sixteen microscopic images containing single eggs of 16 different types of parasites. For experiment images were rotated from 0 to 165^0 in steps of 15^0 with 15 different scales	Fertilized Ascaris Lumbricoides, Unfertilized Ascaris Lumbricoides, Diphyllobotrium Latum, Enterobius Vermicularis, Fasciola Hepatica, Hymenolepsis Diminuta, Hymenolepsis Nana, Kellicoti, Kellicoti, Schistosoma Haematobium, Giardia Lamblia, Schistosoma Japonicum, Schistosoma Mansoni, Schistosoma Mansoni, Trichuris Trichura and Hookworm
Derya Avci et al. [34], 2009	Sixteen microscopic images containing a single egg of 16 different types of human parasites. For the experiment images were rotated from 0^0 to 165^0 in steps of 15^0 with 10 different scales	Fertilized Ascaris Lumbricoides, Unfertilized Ascaris Lumbricoides, Trichuris Trichura, Diphyllobotrium Latum, Enterobius Vermicularis, Schistosoma Mansoni, Fasciola Hepatica, Giardia Lamblia, Hymenolepsis Diminuta, Hookworm, Kellicoti, Paragonimus Westermani, Schistosoma Haematobium, Hymenolepsis Nana, Schistosoma Japonicum, Taenia Saginata
S. M. Sulong et al. [37], 2012	Microscopic images containing parasite eggs and other feces artifacts	Ascaris Lumbricoides

Table 2.1: (Continued)

Paper	Type of Images	Species of Parasite eggs
Alicia Alva et al. [35], 2017	Microscopic images of fecal smears containing single parasite egg	Taenia sp., Trichuris trichiura, Diphyllobothrium latum, and Fasciola hepatica
J. M. Bruun [36], 2014	100 microscopic images containing multiple parasite eggs, captured under brightfield and darkfield in liquid suspension and	Trichuris suis
S. V. Inacio et al. [40], 2020	Microscopic fecal sample images containing multiple parasite eggs and cysts	Eggs of Canine Gastrointestinal parasite: Toxocara spp., Ancylostoma spp., Trichuris spp., and Giardia spp
A. E. Abdalla [39], 2017	4402 images of only parasite eggs of 7 Eimeria species in chickens and 2902 of 11 Eimeria species in rabbits	E. Acervulina, E. Brunetti, E. Maxima, E. Mitis, E. Necatrix, E. Praecox, E. Tenella, E. Coecicola, E. Exigua, E. Flavescens, E. Intestinalis, E. Irresidua, E. Magna, E. Media, E. Perforans, E. Piriformis, E. Vejdovskyi, E. Stiedai

2.1.2 Edge Detection Based Approaches

Edge detection of different objects in an image involves measuring the discontinuity or sudden changes of pixel intensity in the image [25, 41]. Edges of different objects in an image are the local or regional change of pixel intensity [42]. Detection of edges helps in understanding the shape of the objects present in images. Many applications like biometrics, medical image analysis, object detection, etc., use various edge detection methods for identifying meaningful patterns [25]. There are many different types of edge detection approaches, but the effectiveness of a method mostly depends on the applications and type of images being used. Usually, most edge detection techniques use thresholding or gradients of pixel intensi-

ties to detect the edges [43]. Most of the classical methods apply two-dimensional filters or operators that are sensitive to large gradients that convolve over the entire image to detect the edges of various objects [44]. Among all the available edge detectors, Sobel, Canny, Roberts, Prewitt, and Laplacian of Gaussian (LoG) are the most commonly used operators [43–45]. These edge-detection methods have been used in various research works related to the automatic segmentation of parasite eggs in microscopic images, and it is found to be very effective. Various works in this area that used edge detection-based methods are discussed below.

In 2012, R. S. Hadi et al. [2] used an edge detection method based on the canny operator for the segmentation of microscopic images containing parasite eggs namely Ascaris lumbricoides and Trichuris trichiura. The images used in their work contained multiple parasite eggs as well as fecal impurities or non-egg objects. The brightness, contrast, and sharpness of the images were enhanced so that the edge detection process could effectively detect the edges of different parasite eggs and other objects. This work was extended by K. H. Ghazali et al. [46], where the authors analyzed the effectiveness of different edge detection operators such as Canny, Sobel, Prewitt, Roberts, and LoG for segmentation of the same two types of parasite eggs. They also analyzed the usefulness of different pre-processing methods like noise reduction using a median filter, enhancement of image contrast, and edge sharpness in the process of edge detection. K. Ray et al. [47] also used the canny edge detection technique in the process of parasite egg segmentation in microscopic images of fecal samples. To properly detect all the parasite eggs and other objects in the images, two pre-processing steps, such as noise removal and contrast enhancement, were applied. The final segmentation process of the images was carried out by applying some morphological operations, viz., dilation, erosion, and filling holes in the edge-detected images. Later, some unwanted objects were eliminated based on their shape (circularity) and size in the segmented images. Roxona Flores-Quispe et al. [48–50] mentioned that the Sobel operator is less sensitive to image noise than other edge detection operators, and hence, they used it to detect the edges of eight different types of human parasite eggs. In this work, the operator was applied to the RGB images of parasite eggs along the vertical and horizontal axes in each channel.

There are a few works that used some additional operations after the edge detection process. Circular Hough Transformation (CHT) [51] is one of the most commonly used operations among those operations. CHT helps in finding circular objects, and it has been used successfully for detecting various types of parasite eggs in the images. K. Ray et al. [10] used the Circular Hough Transformation

[51] for segmentation of microscopic fecal sample images containing two types of parasite eggs that were also used in [47]. In this work, the CHT operation was applied to the edge-detected images produced by the Canny operator. Some pre-processing steps, such as noise reduction, brightness, and contrast enhancement, were also used before edge detection. It is observed that the CHT helped in detecting the overlapped parasite eggs and other objects in the images, which cannot be achieved using traditional segmentation methods. Oscar T. Nkamganga et al. [52–54] also used CHT after applying canny edge detection operation for segmentation of parasite egg images. In their work, they performed another operation called Distance Regularized Level Set Evolution (DRLSE) for contour optimization and extraction of the detected parasite eggs from the images.

2.1.3 Edge Detection using Wavelet Transform

A wavelet transform can also be used to detect the edges of different objects in the images. The wavelet transform is the analysis of signals using a function that has wave-like oscillation with a zero mean and exists for a finite duration, called a wavelet [55, 56]. It has been found that the wavelet transform is very useful in analyzing image contents as well as detecting edges effectively. An example of an edge detection approach using a wavelet transform can be found in [56]. Classical gradient and Laplacian-based methods have some limitations, such as complex computation, sensitivity to noise, and localization error on the curve edges [56, 57]. The wavelet transform can overcome most of these limitations and perform better edge detection [57]. There are a few works where wavelet transform-based approaches are used for detecting the edges of various parasite eggs in microscopic images.

In 2014, Daniel Tchiotsop et al. [55] developed a segmentation approach using multiscale wavelet transform to detect the edges of parasite eggs in stool microscopic images. First, the image smoothing was performed using the Gaussian function, and wavelet transform was carried out in multiple scales to detect various sizes of edges. During their experiment, they observed that the variation of the threshold value and scaling factor in the wavelet transform yields various structures of different sizes and shapes, like the cell nucleus, cytoplasm membrane, operculum, etc. [55]. The authors stated that the proposed edge detection approach performed better than other classical methods like Canny, Sobel, Roberts, and Prewitt on the parasite egg images in their database. B. S. Tchinda et al. [58, 59] also used a multiscale wavelet transform-based technique to detect the

edges of nine different species of human intestinal parasite eggs. After the edge detection, the circular hough transform [51] was applied to detect the round-shaped objects. Finally, an active contour model (ACM) [60] based on a gradient vector flow was applied with the edges obtained by the CHT as initial contours. The parasite eggs were segmented out using the logical operation between the segmentation masks obtained from the final step and the corresponding original images. Various parasite egg segmentation works that used edge detection-based techniques are recorded in Table 2.2.

Table 2.2: Parasite egg segmentation works that used Edge detection-based methods

Paper	**Type of Images**	**Species of Parasite eggs**
R. S. Hadi et al. [2], 2012	200 microscopic fecal sample images containing parasite eggs of each and debris	Ascaris lumbricoides ova and Trichuris trichiura ova
K. H. Ghazali et al. [46], 2013	200 microscopic fecal sample images containing parasite eggs of each and debris	Ascaris lumbricoides ova and Trichuris trichiura ova
R. F. Quispe et al. [48–50], 2014, 2019	2053 microscopic images of eight species of human parasite eggs. Each image only has one single parasite egg	Ascaris, Enterobius-Vermicularis, Uncinarias, Taenia-Solium, Trichuris, Dyphillobothrium-Pacificum, Fasciola Hepatica
K. Ray et al. [10, 47], 2019, 2021	1000 microscopic images of fecal samples of pigs containing multiple types of parasite eggs and fecal impurities	Ascaris lumbricoides, Necator americanus

Table 2.2: (Continued)

Paper	Type of Images	Species of Parasite eggs
O. T. Nkamganga et al. [52–54], 2018, 2019	1240 microscopic images of 20 species of parasite eggs. Each image contains a single egg and debris	Entamoeba histolytica cyst, Entamoeba coli cyst, Clonorchis sinensis egg, Trichuris trichura egg, Balantidium coli cyst, Iodamoeba butschlii trophozoite, Diphyllobothrium latum egg, Chilomastix mesnili cyst, Hymenolepis nana egg, Schistosoma mansoni egg, Schistosoma haematobium egg, Heterophyes heterophyes egg, Ascaris lumbricoides egg, Giardia lamblia Cyst, Fasciola hepatica egg, Blastocystis hominis egg, Paragonimus westermani egg, Entamoeba histolytica trophozoite, Taenia solium egg, Ancylostoma duodenale egg.
B. S. Tchinda et al. [58], 2015	540 microscopic stool images containing nine types of human intestinal parasite eggs and some impurities	Balantidium Coli, Endolimax Nana, Entamoeba Coli, Entamoeba Hartmanni, Entamoeba Histolytica, Entamoeba Polecki, Giardia Lamblia, Iodamoeba Butschlii, Chilomastix Mesnili.

Table 2.2: (Continued)

Paper	Type of Images	Species of Parasite eggs
B. S. Tchinda et al. [59], 2019	1800 microscopic feces images of containing 15 types of human helminthes eggs and amoeba cysts and impurities	Nine types of protozoan cysts: Giardia lamblia, Entamoeba hartmanni, Entamoeba polecki, Entamoeba histolytica, Entamoeba coli, Endolimax nana, Balantidium coli, chilomastix mesnili, Iodamoeba Butschlii and six types of helminthes eggs: Ascaris, Tapeworm, Schistosoma mansoni, Schistosoma intercalatum, Schistosoma japonicum, whipworm

2.1.4 Active Contour Model (ACM)-based Approaches

Active Contour Model (ACM) or Snake was introduced by Michael Kass et al. [60] in 1988. Since then it has been widely used in various applications of computer vision such as object tracking, edge detection, shape recognition, and stereo matching [60]. ACM uses the principle of energy optimization to portray object boundaries or edges in the images [61]. It is seen that many researchers are actively using this model in various medical image segmentation processes. As described in the work by Michael Kass et al. [60], the original ACM or snake uses a user-defined initial contour position along with an energy function to perform segmentation [61]. The energy function can be formulated from the internal and external forces computed from the images. Then the segmentation process can be achieved by moving the snake around the image domain by optimizing the energy functions [61,62]. Details about the snake, its energy functions, and their working principles can be broadly studied in [60,61]. A few works that used the ACM in parasite egg segmentation are mentioned below.

Rema M. and Madhu S. Nair [62] used a region-based Active Contour Model for the segmentation of intestinal parasite eggs in bright field microscopic images. The energy function for their proposed model was formulated using the lo-

cal information of various regions in the input images. They stated that the active contour models that use the energy functions computed from global image statistics are not useful enough to segment objects with heterogeneous backgrounds. This problem was handled by analyzing the local regions and constructing some local energies [62]. The initial contours for the proposed ACM model were achieved by thresholding the input images, followed by morphological opening operation. The authors of this work mentioned that the threshold value calculated using Otsu's method yields poor binary images. Hence, they experimented using different threshold values ranging from 0.20 (20%) to 0.55 (55%) of gray pixel intensity level and selected the value of 0.40 (40%) that produced the best segmentation result for all the images in their database. J. Zhang et al. [63] also used an ACM for automatic segmentation of Schistosoma japonicum eggs in microscopic fecal sample images. As the first step of the segmentation process, they enhanced the boundaries of the eggs in the original images by the Random-Like Feature [64] method. Then a threshold value (*threas*) was obtained from each of these images using the Equation 2.2 and applied binary thresholding (B) on them as shown in Equation 2.3.

$$threas = T_{min} + (T_{max} - T_{min})\lambda \tag{2.2}$$

$$B = \begin{cases} 1, & \text{if } T > threas \\ 0, & \text{if } T \leq threas \end{cases} \tag{2.3}$$

Where T represents an enhanced image, T_{max} is the maximum intensity, T_{min} is the minimum intensity, λ is a ratio parameter for choosing the threshold value [63] and B is the final binary image. The obtained segmented images were further processed by thinning and connected component analysis to reduce noise and unwanted structures. Then a method called Randomized Hough Transform [65] was applied to these images to extract the boundaries of elliptical-shaped parasite eggs. These ellipse edge points were used as initial points for the active contour model to accurately segment the parasite eggs in the images. B. S. Tchinda et al. [58, 59] also used an ACM-based approach for segmentation of different parasite eggs where the edges of various objects are detected using wavelet transform and CHT as discussed in the Section 2.1.3. Different types of parasite eggs and images used in these works can be viewed in Table 2.3.

Table 2.3: Parasite egg segmentation works that used ACM-based methods

Paper	Type of Images	Species of Parasite eggs
Rema M. et al. [62], 2013	Bright-field microscopic images of fecal samples containing human intestinal parasite eggs and fecal impurities. The number of images used in the experiment was not specified	Not specified
J. Zhang et al. [63], 2014	116 microscopic images of fecal samples containing two types of parasite eggs	Schistosoma japonicum, Clonorchis sinensis
B. S. Tchinda et al. [58, 59], 2015, 2019	1800 microscopic feces images containing 15 types of human helminthes eggs and amoeba cysts and impurities	Nine types of protozoan cysts: Giardia lamblia, Entamoeba polecki, Entamoeba histolytica, Entamoeba hartmanni, Entamoeba coli, Balantidium coli, Endolimax nana, Iodamoeba Butschlii, Chilomastix mesnili and six types of helminthes eggs: Ascaris, Schistosoma mansoni, Tapeworm, Schistosoma japonicum, whipworm, Schistosoma intercalatum

2.1.5 Watershed Algorithm-based Segmentation

Watershed segmentation is a type of region-based method that uses morphological characteristics of images [66]. After introducing an algorithm based on watershed transform by Vincent and Soille in 1991, it has been widely used in various image segmentation applications [67]. The concept of the watershed lies in the visualization of image gray levels in a topographic representation where bright pixels represent ridges and dark pixels as valleys [66–68]. Conceptually, there are two notions viz: catchment basin that represent image regions or valleys and ridge lines or watershed lines, which represent region boundaries. Suppose a hole is punched at each of the local minima of the regions or valleys and pour water through these holes, the water will slowly rise and fill the valleys, and eventually

at a point water from two separate regions will merge. However, water from two separate regions is not allowed to mix, and therefore the algorithm built a dam or watershed line between two catchment basins or regions [66]. The algorithm continues flooding the entire image until it segments the whole surface into multiple different catchment basins separated by watershed lines. Here we have discussed a few segmentation approaches that used watershed-based methods in automatic parasite egg detection-related works.

C. T. N. Suzuki et al. [27,69] applied an Image Foresting Transform (IFT)-based watershed algorithm for segmentation of fifteen different types of human helminth parasite eggs, protozoan cysts, and larvae from microscopic images of fecal samples. Global thresholding operation was performed on the images using manually determined threshold values as the initial step of their segmentation process. Here, two threshold values were selected: one for the images of cysts and larvae, and another for the eggs. Then an ellipse matching method was applied to extract the elliptical-shaped objects from the thresholded binary images. Internal and external markers were created using erosion and dilation operations on the detected elliptical-shaped objects. These markers were then used by the IFT-based watershed algorithm to produce the final segmentation masks. A similar kind of approach was adopted by D. Osaku et al. [70] where they also used an IFT-based watershed algorithm with only binary thresholding for segmentation of fifteen common species of human intestinal parasite eggs.

B. Jimenez et al. [71] used a watershed algorithm with distance field transform to separate the overlapping objects in the segmentation process of helminth eggs from microscopic images of wastewater samples. The authors applied some pre-processing steps such as image smoothing using a low pass filter and contrast enhancement. Detection of various objects in the images was performed using median filtering, histogram equalization, edge detection, distance transformation, and watershed algorithm [71]. Subsequently, they developed two modified versions of their proposed approach to improve performance. The segmentation method in the final version starts with calculating the average gray-level profiles of various objects and the mean gray value of the image background. Then a threshold value was calculated from the mean gray value of the background and the standard deviation as shown in equation 2.4 [71]. In the thresholding operation, a pixel was considered part of an object only if the value of that pixel was lower than the threshold value. Finally, the distance transform followed by the watershed algorithm was applied to separate the overlapping objects and improve the identification rate. The Table 2.4 present the type of images and parasite eggs

that used watershed algorithm for segmentation.

$$Threshold = Background_{mean} - Std_{Background} \tag{2.4}$$

Where $Background_{mean}$ represents the mean gray level value of background and $Std_{Background}$ is the background standard deviation, calculated as the equations 2.5 and 2.6.

$$Background_{mean} = \frac{1}{N} \sum_{i=majoraxis}^{N} P_{average}(i), \tag{2.5}$$

$$Std_{Background} = \frac{1}{N} \sum_{i=majoraxis}^{N} (P_{average}(i) - Background_{mean})^2 \tag{2.6}$$

In the above equations, $P_{average}$ represents the average gray-level profile of an object.

Table 2.4: Parasite egg detection works that used Watershed-based methods

Paper	**Type of Images**	**Species of Parasite eggs**
C. T. N. Suzuki et al. [27, 69], [62], 2013	Bright field microscopic images of 15 types of human intestinal parasite eggs with fecal impurities	Ascaris lumbricoides, Ancylostomatidae, Enterobius vermicularis, Trichuris trichiura, Hymenolepis diminuta, Hymenolepis nana, Taenia spp., Strongyloides stercoralis larvae, Schistosoma mansoni, Cysts: Entamoeba histolytica/E.dispar, Entamoeba coli, Giardia duodenalis, Endolimax nana, Blastocystis hominis, Iodamoeba butschlii

Table 2.4: (Continued)

Paper	Type of Images	Species of Parasite eggs
D. Osaku et al. [70], 2020	Microscopic images of fecal samples containing 15 different types of parasite eggs and fecal impurities	Strongyloides stercoralis, Hymenolepis nana, Hymenolepis diminuta, Ancylostomatidae, Enterobius vermicularis, Ascaris lumbricoides, Trichuris trichiura, Schistosoma mansoni, Taenia spp., Entamoeba coli, Entamoeba histolytica / E. dispar, Endolimax nana, Giardia duodenalis, Iodamoeba bütschlii, Blastocystis hominis
B. Jimenez et al. [71], 2016	720 microscopic images of seven species of helminth eggs obtained from the samples of wastewater, sludge, and excreta.	Ascaris lumbricoides-fertilized and unfertilized, Toxocara canis, Trichuris trichiura, Taenia saginata, Hymenolepis diminuta, Hymenolepis nana and Schistosoma mansoni

2.1.6 Clustering-based Segmentation Approaches

Clustering-based algorithms are used to make groups of different data points that have similar properties or features [72]. This characteristic of clustering algorithms can be used in the image segmentation process, where pixels belonging to similar objects can be grouped and separated them from others. It is seen that in many cases, clustering-based image segmentation methods produce better results than classical techniques such as binary thresholding and edge detection [73]. Although there are many different clustering algorithms, such as Fuzzy-C means, DBSCAN, Agglomerative Clustering, Gaussian Mixture Model, etc, it is seen that K-means is the most commonly used clustering algorithm for image segmentation [72, 73]. K-means clustering method partitioned the available data points into K number of clusters. The algorithm chooses K number of cluster centers and calculates the distance of each data from those centers. A data point is assigned to that cluster center from which the distance is minimal.

Although the clustering-based image segmentation method is popular in many applications, there are only a few works that used this method in the area of parasite egg segmentation. It is found that Norhanis A. A. Khairudin et al. in [74, 75] used the K-means clustering-based method for segmentation of parasite egg images. 100 Microscopic images of two types of human intestinal parasite eggs namely Ascaris Lumbricoides and Trichuris Trichiura were used in their experiment. The authors mentioned that each of the images contains a single egg with no other significant impurities or non-egg objects. They also segmented the same images using binary thresholding with Otsu's [38] threshold value and it is observed that the results were very similar to the clustering-based method.

2.1.7 Ellipse Matching-based Approaches

A study shows that most of the parasite eggs are nearly round or elliptical. Hence, many researchers applied different ellipse matching methods to effectively detect various types of parasite eggs from microscopic images that are elliptical. An ellipse matching method can be used on binary images after performing some classical image segmentation operations such as thresholding, edge detection, etc. In many cases, it has been seen that ellipse matching methods are applied directly to grayscale images to detect elliptical-shaped objects. Several works used this method effectively to detect various types of parasite eggs in different kinds of images, and below we have discussed some of those works.

As mentioned in Section 2.1.4, J. Zhang et al. [63] used a randomized hough transform [65] based ellipse matching method to detect the edges of various elliptical-shaped parasite eggs and other similar objects in the images. The original microscopic images were segmented using the binary thresholding method, and the ellipse matching method was applied to the output binary images. The contours of various objects obtained from the ellipse matching were further used for an active contour model for accurate segmentation of the parasite eggs. In another work from C. T. N. Suzuki et al., [27], an ellipse matching method was also applied to the binary thresholded images containing various types of parasite eggs and non-egg objects. The ellipse matching method produced markers that were used in the watershed algorithm for the final segmentation of the objects. J. M. Burrn et al. [76] also used an ellipse matching method by constructing an elliptical filter based on the width and length of Trichuris suis eggs in bright field microscopic images. They applied the method directly to the grayscale images of the mentioned parasite eggs. Zhxiun Li et al. [77] mentioned an approach for the

detection of six types of human parasite eggs using the ellipse matching method. Their segmentation pipeline consists of several steps, as follows: Otsu's binary thresholding was performed on the original images to separate the foreground and background objects. A morphological operation was applied to the thresholded images to remove the unwanted objects or debris. Then a phase consistency [78] and zero crossing method-based frequency domain model were applied to detect the boundary edges of the parasite eggs. Finally, an ellipse fitting method was employed to extract the actual oval-shaped parasite eggs and separate them from other non-egg objects in the images. Types of parasite eggs and images used by these works are mentioned in Table 2.5.

Table 2.5: Works that used Ellipse matching-based methods

Paper	**Type of Images**	**Species of Parasite eggs**
J. M. Burrn et al. [76], 2012	24 bright field and dark field microscopic images containing multiple parasite eggs	Trichuris suis eggs.
J. Zhang et al. [63], 2014	116 microscopic image of fecal samples containing two types of parasite eggs	Schistosoma japonicum, Clonorchis sinensis.
C. T. N. Suzuki et al. [27], 2013	Bright-field microscopic images of 15 different types of human intestinal parasite eggs with fecal impurities	Ascaris lumbricoides, Enterobius vermicularis, Trichuris trichiura, Ancylostomatidae, Hymenolepis nana, Taenia spp., Hymenolepis diminuta, Schistosoma mansoni, Strongyloides stercoralis larvae, Cysts: Entamoeba histolytica/E.dispar, Giardia duodenalis, Entamoeba coli, Endolimax nana, Iodamoeba butschlii, Blastocystis hominis.
Zhxiun Li et al. [77], 2015	1179 images of fecal samples containing multiple parasite eggs and fecal impurities	Blood fluke, liver fluke, Pinworm, Whipworm, fertilized and non-fertilized roundworm.

2.1.8 Segmentation using Convolutional Neural Network (CNN) models

The recent advancement of different techniques in computer vision led the researchers to use convolutional neural network (CNN) based methods in various applications of classifications, object detection, and image segmentation. CNN was primarily developed for image classification and was later employed in semantic segmentation. In recent years, researchers have used CNN to develop various semantic and instance segmentation models that have proven effective in a variety of applications such as robotics, self-driving cars, and so on. Among the various approaches, Fully Convolutional Network (FCN) [79], U-net [80], and encoder-decoder [81, 82] are the most popular that used in various image segmentation applications such as medical image analysis, scene understanding, and remote sensing. FCN was introduced by Jonathon Long et al. [79] for semantic segmentation of images by utilizing only the convolutional layers of a CNN architecture. Encoder-decoder-based architecture is introduced by Hyeonwoo Noh et al. [82] using de-convolution or transposed convolution layers. The architecture consists of an encoder part that uses convolution layers and a decoder part which is a mirrored version of the encoder part. The encoder generates multidimensional feature maps using convolution, pooling, and rectification operations. The decoder part consists of multiple de-convolution, un-pooling, and rectification layers that generate the object segmentation mask from the features generated by the encoder. Another popular model named U-net was introduced by Olaf Ronneberger et al. [80] biomedical image segmentation. Similar to FCN architecture, U-net also consists of only fully convolutional layers that produce segmentation masks from an input image. It also contains a contracting or down-sampling path that captures the context information and an expanding or up-sampling path for localization of the objects [80]. Some of the major works on parasite egg detection that used CNN-based segmentation methods are discussed below.

Adedotun Akintayo et al. [83, 84] mentioned an approach called convolutional selective autoencoder which was based on the encoder-decoder architecture for the detection of Soybean Cyst Nematode (SCN) eggs in microscopic images of soil samples. The images used in their experiment contain multiple SCN eggs along with other non-egg objects, and hence the model is trained with multiple labeled patches of smaller sizes that are extracted from the original images. The encoder part of the model captures some meaningful features from the input images using the convolutional layers, and the decoder part reconstructs the patterns of interest (only the SCN eggs) in the output segmentation masks [84]. The developed model

scans each patch one by one and discards those where an SCN egg is not fully present and centered on it. This way, they selected only the positive patches that contained a full SCN egg for training the classifier. Patryk Najgebauer et al. [85] applied an FCN-based architecture for the segmentation and detection of four different types of parasite eggs. Images used in their work are annotated with seven classes of objects that include four types of parasite eggs and three classes of other objects such as air bubbles, backgrounds, and pollution. These annotated ground truths are used for training the FCN model, which outputs colour segmentation masks indicating the different objects and parasite eggs.

A U-net-based model is used by Marc Górriz et al. [86] for segmentation of leishmania parasites. The images are annotated, indicating seven classes of objects: amastigote, promastigote, adhered parasite, cytoplasm, nucleus, background, and unknown. The patches of size 224×224 pixels are extracted from the original training images, which are used to train the U-net model. The work used overlapping patches in the training to detect some overlapping objects in the images. To address the issue of high-class imbalance during training, a two-stage non-uniform sampling strategy is adopted for selecting the different patches. The first few training iterations used patches with at least 40% pixels belonging to any of the three classes, namely amastigote, promastigote, or adherent, while the remaining iterations utilized a uniform sampling strategy over all patches [86]. Yaning Li et al. [87] also used a U-net-based model to segment five different types of parasite eggs, viz., Trichuris spp., Strongyle, Toxocara spp., Isospora, and Eimeria in microscopic images of animal fecal samples. The authors modified the original U-net design by rearranging several convolutional and max-pooling layers according to their requirements. Ideal Oscar Libouga et al. [88] applied a similar approach for the segmentation of Ascaris Lumbricoides, Schistosoma mansoni, Trichuris Trichiura, and Oxyure eggs. They trained the model with colour images so that it could take advantage of the colour information and yield better output. As a result, it detected the various parasite eggs with an overall accuracy of 99.8%. Prosper Oyibo et al. [89] used a two-stage approach for the segmentation of S. haematobium parasite eggs in microscopic images of urine samples. The first stage utilized a deep CNN model named DeepLabv3-MobilNetev3 that performs semantic segmentation on the images, while the next stage uses the ellipse fitting method to detect elliptical-shaped objects as well as overlapping parasite eggs. The proposed approach showed 93.75% sensitivity, 93.94% specificity, and 93.75% precision in detecting the mentioned parasite egg.

Table 2.6: Parasite egg segmentation/detection works that applied Convolutional Neural Network-based methods

Paper	**Type of Images**	**Species of Parasite eggs**
A. Akintayo et al. [84], 2018	644 microscopic soil sample images containing parasite eggs and non-egg particles	Soybean Cyst Nematode eggs
M. Górriz et al. [86], 2018	45 bright field microscopic images obtained from macrophage infection of RAW cells with Leishmania infantum, Leishmania major and Leishmania braziliensis that shows the shape of parasites before and after infecting the cells	Leishmaniasis Parasite
Yaning Li et al. [87], 2019	951 microscopic images of fecal samples of animals containing parasite eggs as well as debris	Trichuris spp. (monkey), Strongyle (sheep), Toxocara spp. (dog), Isospora (dog), Eimeria (cow) and Eimeria (sheep)
P. Najgebauer et al. [85], 2019	465 images that contain four classes of parasite eggs along with fecal impurities	Whipworms, Visceral worms, Pinworm, Hookworm
Ideal Oscar Libouga et al. [88], 2022	Image dataset contains 320 microscopic images of four types of intestinal parasite eggs. Each image has single or multiple parasite eggs and fecal impurities	Ascaris Lumbricoides, Schistosoma mansoni, Trichuris Trichiura, and Oxyure
Prosper Oyibo et al. [89], 2023	Dataset contains 12,051 images with 17,799 annotated S. haematobium parasite eggs in 2997 images. The dataset consists of images with and without artifacts such as air bubbles, glass debris, etc.	S. haematobium eggs

It is notable that, medical imaging often faces challenges such as noise and varying illumination, which can degrade the quality of diagnostic information. These challenges can obscure key pathological details, leading to misdiagnosis or reduced diagnostic confidence, particularly in modalities like microscopy and X-ray imaging, where fine details are crucial. Effective handling of these issues ensures that diagnostic algorithms can extract meaningful features, even in suboptimal imaging conditions, thus enhancing their performance across diverse clinical scenarios. Recent studies have explored methods such as deep learning-based denoising models, which are particularly effective for removing electrical and environmental noise from medical images. For instance, a study demonstrated how these models could enhance spectral contrast in optoacoustic imaging, significantly improving image clarity and diagnostic capabilities [90].

Dealing with varying illumination conditions is equally important. Models that incorporate adaptive learning mechanisms and multi-scale features have been developed to address this issue, ensuring that critical details are preserved despite inconsistent lighting. Furthermore, combining these methods with neural networks like U-Net or GAN-based frameworks has proven to enhance robustness against artifacts and variations, as demonstrated in recent advancements in tumor segmentation and other diagnostic tasks [90, 91].

2.2 Feature Extraction and Classification of Parasite Egg

Many different types of image features, such as shape, size, texture, etc., can be extracted from the images and used in a classification algorithm for the identification of different types of parasite eggs. There are several well-known machine learning-based classifiers, including ANN, SVM, KNN, Decision Tree, etc., that are used in different works in this field. In this section, we have discussed the features and classification algorithms used in some major works on automatic detection and identification of parasite eggs in microscopic images.

Yang et al. [9] used a two-stage artificial neural network (ANN) approach to automatically identify the seven species of human helminth eggs from microscopic images of stool samples. The detected objects are first classified by ANN-1 as either parasite eggs or non-egg artifacts. In the second stage, the identified parasite eggs are classified into their respective classes. The work used four image

features based on three characteristics, such as size, shape, and eggshell. These features are calculated as follows:

1. $F_1 = \min(r(\theta))/\max(r(\theta))$
   Where $r(\theta)$ is the radial distance of the object's boundary, which is normalized by its mean value [9].

2. $F_2 = \frac{\sum_0^{\pi/4} |R(\omega)|}{\sum_{\pi/4}^{\pi} |R(\omega)|}$; the ratio of low-frequency components to high-frequency components from the magnitude of discrete Fourier transform of $r(\theta)$ and $|R(\omega)|$ [9].

3. $F_3 = \sigma_r$; the standard deviation of $r(\theta)$.

4. $F_4 =$ Total number of pixels in an object.

Dogantekin et al. [33] used Hu's seven invariant moments-based features to identify sixteen different types of human parasite eggs. They used an adaptive network-based fuzzy interface system (IM-ANFIS) for their classification stage, which combines the concepts of fuzzy logic systems with artificial neural networks. The model consists of an ANN learning algorithm and if-then rules. Hu's seven invariant moments were also used in a similar work by Avci and Varol [34], where they adopted a multi-class support vector machine (MC-SVM) classifier for the identification of sixteen types of parasite eggs.

Bruun et al. [76] stated a vision-based method for identifying Trichuris suis parasite eggs in bright field microscopic images. The work extracted two numerical features, longitudinal anisotropy and mean scattering intensity, from the segmented images. Longitudinal anisotropy is the measure of the "linearity" of the egg contents along the length of the egg vs. across the egg [76]. It is calculated as the ratio of the intensities of the longitudinal and transverse autocorrelations of the egg content. Mean scattering intensity is calculated as the average grayscale pixel intensity of the egg contents under dark field illumination [76]. They used two classification methods: Linear Discriminant Analysis (LDA) and Quadratic Discriminant Analysis (QDA).

Hadi et al. [2, 46] extracted the area, length, width, size of boundary, and circularity of object as features automatically identifying Ascaris lumbricoides and Trichuris trichiura eggs. A logical classification method known as the threshold with logical classification method (TLCM) was employed for the classification task. The method works in such a way that objects that do not fall within the range of each feature type are eliminated at each iteration.

To automatically identify fifteen different types of human intestinal parasite eggs in microscopic images of fecal samples, Celso T. N. Suzuki et al. [27] analyzed the results of three classification methods: ANN, SVM, and Optimum-Path Forest (OPF). They used twelve different features, namely: 1) Ellipticity, a measure of how similar an object is to an elliptical shape, is calculated by dividing the area of the best-fitted ellipse by the area of the candidate object; 2) Geodesic distance ratio, which is derived by dividing the length of the longest geodesic path through the object by the length of the shortest geodesic path; 3) Curvature variance; 4) Salience variance, which is defined as the largest area between the internal and external regions of object's contour; 5) Red texture, which is the total number of pixels of an area calculated from a closing operation; 6) Red average value, which is average pixel value in the red bend; 7) Average number of regional minima in the gradient image inside the object; 8) Object's perimeter; 9) Object area; and 10) Second, third, and fourth-order image moments representing variance, skewness (symmetry), and kurtosis. In their other work [69], object area, perimeter, symmetry, major and minor axes of the best-fit ellipse within the object, the difference between the ellipse and the object, energy, entropy, variance, and homogeneity of the co-occurrence matrix are used as features along with the OPF classifier for identifying fifteen types of ectoparasites found in Brazil.

Gökhan Şengül [92] used texture-based features computed from a gray-level co-occurrence matrix (GLCM) [29] and a kNN classifier for the identification of fourteen types of human parasite eggs. A GLCM, the matrix computed from a gray-scale image and then converted to a row vector with a size of $1 \times (M \times N)$, which is directly used as the feature set for the respective image. GLCM texture-based features, along with a few shape-based features, are also used by Zhixun Li et al. [77] for identifying six different types of human parasite eggs. Texture features included in their work are contrast, energy, identity, relevance, gray mean, variance, and entropy. Shape-based features include circularity or roundness, average normalized radial length that represents the distance between the points on the edge and center of the egg, needle-like degree (Spicu), which is computed as F_2 from the work of Yang et al. [9], number of bulges in parasite egg using local maxima and minima, and elliptic normalized skeleton, which is the number of points on the contour [77]. They trained an SVM classifier using the extracted features to categorize the parasite eggs. B. Jimenez et al. [71] proposed a system to identify seven species of human helminth eggs in microscopic images of wastewater. In their work, they used a Naive Bayesian classifier with shape-based features of parasite eggs, including area, perimeter, eccentricity, and texture features such as energy, mean grey level, contrast, correlation, and homogeneity.

They divided their work into three phases, called version 1, version 2, and version 3. In version 1, they considered four classes of parasite eggs, namely Ascaris lumbricoides, Trichuris Trichura, Toxocara canis, Taenia saginata, while in the later two versions, they used three other types of parasite eggs, viz., Hymenolepis nana, Hymenolepis diminuta, Schistosoma mansoni.

Similar kinds of features, including object area, perimeter, major axis length, minor axis length of the best-fitted ellipse, and symmetry, were used by Sandra Valéria Inácio et al. [93] for automatic identification of four types of canine intestinal parasite eggs. They also used co-occurrence matrix-based features such as energy, variance, and homogeneity and trained them using an SVM classifier.

Raw pixel intensity-based features are used in a work by Mohamed A. E. Abdalla and Huseyin Seker [39] for the identification of Eimeria parasites. They extracted three features for every image of size $M \times N$ based on the mean pixel values. The column feature (CF) set is computed from the columns as $CF = [cf_1, cf_2, cf_3, ...], cf_m]$, where $cf_m = \frac{\Sigma_{i=1}^{N} P_{i,m}}{N}$. The row feature (RF) set is computed from the row of the image as $RF = [rf_1, rf_2, rf_3, ...], rf_m]$, where $rf_m = \frac{\Sigma_{i=1}^{M} P_{n,i}}{M}$ and the third set CRF combines both row and column features. Relieff algorithm is used in the extracted feature set to reduce the feature size. For classification, ANN and kNN are used in their work.

Beaudelaire Saha Tchinda et al. [58, 59] stated a method based on probabilistic neural networks (PNN) and principal component analysis (PCA) for the identification of nine types of human parasite cysts in microscopic stool images. The feature vector is extracted using the pixel values of segmented images of size 12×12. PCA analysis is to reduce the feature dimension, and the first two PCA components were considered to be used in the classification algorithm. Oscar Takam Nkamgang et al. [52] used a Histogram of Oriented Gradients (HOG) features with Linear Discriminant Analysis (LDA) and a neuro-fuzzy classifier for automatic identification of various types of human intestinal parasite eggs in microscopic images of fecal samples. LDA was used to reduce the dimension of the extracted HOG features, which were near a thousand, and to select the most prominent features.

Table 2.7: Various types of Features and Classification algorithms used in Automatic Identification of Parasite Eggs

Article	**Types of Features**	**Classification algorithm**	**Number of Classes**	**Obtained Results**
Yang et al. [9], 2001	Object area, standard deviation, ratio of minimum to maximum trajectory of radial distance, ratio of low-frequency to high-frequency components (Fourier Transform)	Two-stage Artificial Neural Network	7	90.3%
Dogantekin et al. [33], 2008	Hu's seven invariant moments	Adaptive network-based fuzzy interface system (IM-ANFIS)	16	95%
Avci and Varol [34], 2009	Hu's seven invariant moments	Multi-Class SVM	16	97.7%
Bruun et al. [76], 2012	Longitudinal anisotropy, mean scattering intensity	Linear Discriminant Analysis and Quadratic Discriminant Analysis	2	93%
Hadi et al. [2, 46], 2012, 2013	Area, length, width, boundary size, circularity	Threshold with logical classification method (TLCM)	2	93% and 94%

Table 2.7: (Continued)

Article	**Types of Features**	**Classification algorithm**	**Number of Classes**	**Obtained Results**
Celso T. N. Suzuki et al. [27], 2013	Ellipticity, geodesic distances, curvature variance, salience variance, red texture, red average value, average number of regional minima, perimeter, area, variance, skewness, kurtosis	ANN, SVM, Optimum-Path Forest (OPF)	15	Sensitivity = 90.38%, Specificity = 98.32%, Efficiency = 98.19%
Celso T. N. Suzuki et al. [69], 2013	Object area, perimeter, symmetry, major and minor axes of best-fit ellipse, difference between ellipse and object, energy, entropy, variance, homogeneity	Optimum-Path Forest (OPF)	15	Sensitivity = 93.00%, Specificity = 99.17%
Gokhan Şengul [92], 2016	Texture-based features from GLCM	K-Nearest Neighbor	14	99%
Zhixun Li et al. [77], 2015	Energy, identity, relevance, gray mean, variance, entropy; shape-based features: circularity, average normalized radial length, needle-like degree, number of bulges, number of contour points	SVM	6	95%

Table 2.7: (Continued)

Article	**Types of Features**	**Classification algorithm**	**Number of Classes**	**Obtained Results**
B. Jimenez et al. [71], 2016	Area, perimeter, eccentricity, texture features: energy, mean grey level, contrast, correlation, homogeneity	Naive Bayes	7	Specificity = 99%, Sensitivity = 80% to 90%
Mohamed A. E. Abdalla and Huseyin Seker [39], 2017	Pixel-based features: column features (CF), row features (RF), combined CF and RF (CRF)	ANN, kNN	7 (chickens), 11 (rabbit)	96.6% (chicken), 91.9% (rabbit)
Oscar Takam Nkamgang et al. [52], 2018	HOG features with LDA	Neuro-Fuzzy Classifier (fuzzy system + ANN)	20	100%
Beaudelaire Saha Tchinda et al. [58, 59], 2015, 2019	PCA projection of pixel values	Probabilistic Neural Networks (PNN)	9, 15	100%, 100%
Sandra Valeria Inácio et al. [93], 2020	Object area, perimeter, major axis length, minor axis length of best-fitted ellipse, symmetry, energy, variance, homogeneity	SVM	4	Kappa coefficient = 0.76

2.3 CNN-based Classification and Object Detection methods used in Parasite Egg Identification

Narut Butploy et al. [94] used CNN for the recognition of Ascaris Lumbricoides eggs in microscopic images of stool samples. The proposed optimal CNN architecture for the classification of three categories of A. lumbricoides eggs, such as infertile eggs, fertile eggs, and decoricate eggs. They trained the model with 200 images of each class and obtained an overall accuracy of 93.33%.

Thanaphon Suwannaphong et al. [95] also proposed a CNN-based model by applying a transfer learning strategy for the classification of four types of parasite eggs in low-quality microscopic images. The approach used a patch-based and sliding window technique to locate the parasite eggs in the images. To locate the parasite eggs, the patch size was set to 100×100 pixels with a patch overlapping ratio of 4:5. To train the classifier, they used 97 images and labelled the patches as egg patches and backgrounds. Data augmentation is applied to increase the size of training samples and eliminate the class imbalance problem. The training process utilized the transfer learning method with fine-tuned hyper-parameters of pre-trained networks, including AlexNet and ResNet50. The author concluded that ResNet50 outperforms AlexNet in the overall recognition of parasite eggs and background. The highest accuracy achieved by AlextNet with patch-based training is 96.93% while ResNet50 achieved 98.25%. However, true positive rate of each class of parasite eggs is not that satisfactory, which ranges from around 56% to 73%.

Convolutional neural network-based object detection models such as Faster-RCNN, YOLO (You Only Look Once), and SSD (Single Shot Detection) are also used in some of the recent works on parasite egg detection. A Faster-RCNN model is used by N. Q. Viet et al. [96] for the detection of eight different types of parasite eggs in microscopic stool images. The authors fine-tuned the hyper-parameters of the original region proposal and classification network of the model and trained it with the annotated parasite egg images. A. Kitvimonrat et al. [97] performed experiments using three different object detectors, viz., Faster-RCNN, CenterNet, and RetinaNet for the detection of two types of parasitic eggs, namely Opisthorchis Vivertini and Minute Intestinal Flukes. The work used ResNet as the backbone network, in all three object detectors with pre-trained weights from ImageNet (for faster RCNN and RetinaNet) and the MS COCO dataset (for Cen-

terNet). Qiaoliang Li et al. [98] used a CNN model called FecalNet to automate the detection of various objects and parasite eggs such as intestinal mucosal epithelial cells, erythrocytes, leukocytes, eggs of whipworms, and Ascaris in fecal microscopic images. They used ResNet152 as the backbone network for their model and a Feature Pyramid Network (FPN) module for the generation of region proposals. Table 2.6 lists the different types of images and parasite eggs used in these works. Satish Kumar et al. [99] used the YOLOv5 object detection algorithm for the detection of five different parasite cysts of size 416×416. The model is trained with 3657 images for 100 epochs and tested with 850 images. Their work achieved approximately 97% mean average precision (mAP) with an average time of 8.8 ms per image.

Table 2.8: Parasite egg Classification and Detection works that applied Convolutional Neural Network-based Approaches

Article	**Approach**	**Type of Images and Dataset Size**	**Species of Parasite eggs**	**Results**
Thanaphon Suwannaphong et al. [95], 2023	Transfer learning with CNN on patches	162 images of size 640 × 480 pixels	Ascaris lumbricoides, Hymenolepis diminuta, Fasciolopsis buski, Taenia spp.	Accuracy = 98.25%
Satish Kumar et al. [99], 2023	YOLOv5 for object detection	5393 images of size 416 × 416 pixels	Hookworm, Hymenolepsis nana, Taenia, Ascaris lumbricoides, Fasciolopsis buski	mAP = 97%
Narut Butploy et al. [94], 2021	CNN based classification	600 images of stool samples (200 each type)	Ascaris (infertile, fertile, decorticate)	Accuracy = 93.33%

Table 2.8: (Continued)

Article	Approach	Type of Images and Dataset Size	Species of Parasite eggs	Results
A. Kitvimonrat et al. [97], 2020	Faster-RCNN, CenterNet, RetinaNet	2654 microscopic images	Opisthorchis Vivertini, Minute Intestinal Fluke	mAP: FRCNN = 0.7394, RetinaNet = 0.6741, CenterNet = 0.5000
Ngo Q. Viet et al. [96], 2019	Faster-RCNN	246 microscopic stool images	Ascaris, Diphyllobothrium, Enterobius, Hookworm, Metagonimus, Schistosoma, Taeniarhynchus, Trichuris	mAP = 97.67%

Recent advancements in deep learning have introduced Vision Transformers (ViTs) as a groundbreaking approach in medical imaging. Vision Transformers, initially proposed by Dosovitskiy et al. [100], leverage self-attention mechanisms to capture long-range dependencies in images, demonstrating exceptional performance in various computer vision tasks, including medical diagnostics. Unlike convolutional neural networks (CNNs), which rely on fixed receptive fields, ViTs divide images into patches and treat them as sequences, enabling the network to learn complex relationships between different parts of the image. This capability is particularly advantageous in medical diagnostics, where subtle differences in visual patterns can indicate critical anomalies.

In the context of parasite egg detection, the adaptability of ViTs to varied shapes, sizes, and noisy backgrounds offers significant potential. Recent studies, such as Liu et al. [101], have demonstrated the superiority of ViTs over traditional

CNNs in biomedical imaging tasks, including histopathology and radiology, where precise identification of irregular structures is crucial. Moreover, ViTs have shown remarkable robustness in working with heterogeneous datasets, making them well-suited for the challenges posed by fecal sample microscopy, which often involves images with debris and artifacts.

Limited labeled datasets have long been a challenge in medical imaging, particularly in tasks such as parasite egg detection, where acquiring annotated data is time-consuming and resource-intensive. Self-supervised learning (SSL) has emerged as a transformative solution to this problem by leveraging unlabeled data to pretrain models on pretext tasks such as image reconstruction or contrastive learning. This approach allows the models to learn robust feature representations, which can be fine-tuned for specific applications. Chen et al. [102] demonstrated that SSL techniques significantly enhance feature extraction in medical imaging, even when labeled data is scarce. Synthetic data generation using Generative Adversarial Networks (GANs), introduced by Goodfellow et al. [103], further addresses these challenges by creating realistic and diverse synthetic images to augment datasets. Studies like Yi et al. [104] have shown that GAN-generated data helps improve model performance by tackling data scarcity and class imbalances. Combining SSL with GAN-based augmentation presents a promising approach for enhancing parasite egg detection in challenging scenarios involving small datasets.

2.4 Conclusion

In this chapter, we present a review of literature related to the automatic detection and identification of parasite eggs in microscopic images. Key insights of the review work are as follows:

- **Sample Preference**: Fecal samples are predominantly used in majority of researches over blood, urine, and tissue samples.
- **Common Species of Parasite Eggs**: Among the various types of parasite eggs, roundworms, hookworms, whipworms, pinworms, and tapeworms are commonly used in many research studies.
- **Traditional Segmentation Methods**:

  - Common techniques include binary thresholding, Canny edge detection, and watershed.
  - Single methods are often inadequate due to challenges like debris and overlapping objects; combining multiple methods may improve performance.
  - A robust segmentation approach applicable to various types of parasite egg images is required for better results.

- **Features and Classification Methods**:
  - The most commonly used features include circularity, object area, ratio of major and minor axis length, Hu moments, and texture features such as energy, entropy, contrast, homogeneity, and mean pixel intensity.
  - SVM, ANN, KNN are the commonly used classifiers for classification of parasite eggs.

- **Deep Learning Advances**:
  - CNN-based classification has been used in several recent work and achieved satisfactory results in identifying different types of parasite eggs.
  - The U-Net has also been employed for segmentation in a few recent studies and has shown effectiveness
  - Faster R-CNN is a popular choice for object detection, yielding good results.
  - These models' performance depends on extensive training samples, precise annotations, and significant computing power.

- **Challenges and Opportunities**:
  - Limited availability of diverse microscopic images restricts research.
  - Many studies use small, homogeneous datasets.
  - There is a need for improved segmentation, feature extraction, and classification methods to effectively detect and identify a wide range of parasite eggs.